# Laser-Assisted Sintering of Silver Nanoparticle Paste for Bonding of Silicon to DBC for High-Temperature Electronics Packaging

# Laser Assisted Sintering of Silver Nanoparticle Paste for Bonding of Silicon to DBC for High Temperature Electronics Packaging

G.D. Liu, C.H. Wang, *Member, IEEE,* and J. Swingler

***Abstract*—This paper presents the development of a laser assisted sintering method of a silver nanoparticle paste for bonding of a silicon chip to a DBC (Direct Bonded Copper) substrate for high temperature electronics packaging applications. The effects of the bonding parameters such as laser power, bonding pressure and time on shear strength were studied. For comparison, samples using hotplate bonding were also produced and studied. Shear strength, cross section and fracture surface analysis were carried out in reliability studies. The results show that shear strength of 10 MPa can be achieved at the bonding pressure of 3 MPa, laser power of 70 W and a very short irradiation time of 1 minute. The shear strength reached 20 MPa when the irradiation time was increased to 5 minutes. The research indicates that the shear strength can be improved by increasing the bonding pressure, laser power and hence the sintering temperature and the irradiation time. The laser assisted method with a short irradiation time of 5 minutes can produce the same level of shear strength as compared with the hotplate-based approach requiring a sintering time of tens of minutes. With the ability of fast and localized heating effect, the laser assisted sintering method can improve the manufacturing efficiency for packaging of high temperature electronics and sensors.**

***Index Terms*—Die attach, laser sintering, silver nanoparticle paste.**

## I. Introduction

High temperature electronic devices and sensors have a wide range of applications in harsh environments, such as deep-drilling equipment, gas turbine engines, aircrafts and space exploration systems. There is a clear need for new assembly and packaging methods for such applications. For high temperature applications, the silicon on insulator (SOI) or the silicon on sapphire (SOS) have been developed by eliminating the leakage effect of the p-n junction using the insulating substrates [1]-[3]. The wide band gap semiconductors, such as silicon carbide (SiC) and gallium nitride (GaN), with excellent electrical characteristics, have been used to fabricate electronic devices and sensors for high temperature operation. It has been reported that the operating temperatures of the SiC and GaN devices are usually higher than 300ºC [4]-[6]. In some cases, the maximum operating temperatures can reach as high as 600ºC [7]. However, in the packaging process, the most commonly used tin (Sn) based solders are not suitable for high temperature applications since the melting points are usually below 250ºC [8]. Although the liquidus points of the lead-tin (Pb-Sn) based solders increase with the content of Pb, the maximum operating temperature is only about 312ºC with 95% of Pb (Pb95-Sn5) [9]. Furthermore, the Pb containing compounds are harmful to human life and the environment. Hence, environmentally friendly lead-free materials with high melting temperatures are required for packaging of high temperature devices.

Glass frit has been an important bonding material for high temperature applications. The glass frit material not only has a high tolerance to the interface roughness, but also can be applied to the requirement of hermetic sealing [10]-[12]. Ahmed Sharif *et al.* [13] proposed a Bi-based lead-free glass frit paste. A silicon die was attached to a ceramic substrate at 430ºC for 10 minutes without any metallization preparation. The shear strength was approximately 20-30 MPa. The joints did not show obvious deterioration after heating at 300ºC for 500 hours. However, the process temperatures in the glass frit bonding are usually much higher than the maximum operation temperatures of the devices, which may cause damage to the devices in the packaging process. Transient liquid phase (TLP) bonding is another important packaging technique for high temperature devices. The TLP bonding process is typically carried out at a temperature between 250ºC and 350ºC, which is slightly higher than the melting point of the lower melting temperature metal in the binary alloy systems. The formed intermetallic compounds would have higher melting points, which means the re-melting temperature of the bonding layer would be higher than the bonding temperature [14]-[16]. Rong *et al.* [17] reported a TLP bonding method at 260ºC for 20 minutes using the electroplated copper (Cu) and tin (Sn). The average shear strength of the bonded structures was 37.5 MPa. Gao *et al.* [18] developed a wafer level Cu-Sn bonding process at 350ºC for 30 minutes for packaging of a high temperature pressure sensor, which can be operated at 300ºC. However, the TLP bonding usually takes a long process time in order to exhaust all the residual liquid phase metal [19].

In recent years, the silver (Ag) nanoparticle paste has

This paragraph of the first footnote will contain the date on which you submitted your paper for review. This work was supported by the UK Engineering and Physical Sciences Research Council (EPSRC, grant EP/R024502/1). (Corresponding author: C. H. Wang)

G.D. Liu and C. H. Wang are with the Institute of Sensors, Signals and Systems, J. Swingler is with the Institute of Mechanical, Process and Energy Engineering, School of Engineering & Physical Sciences, Heriot-Watt University, Edinburgh EH14 4AS, U.K.. (e-mail: g.liu@hw.ac.uk, c.wang@hw.ac.uk, j.swingler@hw.ac.uk )

become a promising material for high temperature die-attach applications. The silver nanoparticle paste is usually produced by dispersing the silver nanoparticle powder in the organic components. The silver nanoparticles (Ag NPs) have attracted much attention not only due to that the sintered nano silver material has a low resistivity of 2.5-10 μΩ·cm and a high thermal conductivity of 200-300 $W(m\cdot K)^{-1}$, but also because the melting point of the sintered silver is near that of the bulk silver at 961ºC, which can meet the requirement for high temperature operation [20]-[23]. The sintering mechanism of the silver nanoparticle could be briefly described using the sphere-to-sphere model and the rapid neck formation process [24]-[26], which indicate the strength of the sintered silver joints depends on the assistant pressure, processing temperature and time. Lei *et al.* [27] sintered a silver nanoparticle paste at 275ºC for 20 minutes with a sintering pressure of 5 MPa and a maximum shear strength of 31.6 MPa was achieved. Buttay *et al.* [28] reported a silver sintering process for power devices. With a purpose designed bonding setup and a sintering pressure of 6 MPa, the silver nanoparticle paste was sintered at 285ºC for 60 minutes and the maximum shear strength was as high as 52.3 MPa. Yu *et al.* [29] proposed a rapid sintering method using a flip-chip bonder. A shear strength of 70.7 MPa was obtained with a higher sintering pressure of 7.6 MPa and a sintering temperature of 300ºC. Although the high sintering pressure and the long sintering time can enhance the bonding quality, the prolonged processing time may reduce the production efficiency and increase the risk of damage to the electronic devices.

In order to overcome the disadvantages of the conventional hot-pressing sintering method, several alternative sintering techniques have been developed, such as laser sintering, spark plasma sintering, and electrical current assisted sintering processes [30]-[32]. Among these techniques, the laser assisted technique has a promising potential to be applied for silver nanoparticle paste sintering due to the advantages of rapid, localized heating effect. Laser-based heating methods have already been used in sub-40 nm semiconductor manufacturing [33]-[35]. In the fields of packaging, Lee *et al.* [36] fabricated light emitting diodes (LEDs) with the laser-sintered silver nanoparticles. For a small chip size of 1.5 mm×1.5 mm, the shear strength was approximately 9 MPa without bonding pressure. In our previous work, for a large chip size of 5 mm× 5mm, Liu *et al.* [37] realized a silicon-silicon (Si-Si) die-attach process using a laser assisted silver nanoparticle sintering method and it was shown a fast process could be achieved in 1 minute. However, the shear strength was only about 5 MPa at a low sintering pressure of 0.2 MPa. Recently, Liu *et al.* [38] realized the Cu-Ag-Cu joints with mixed bimodal size silver nanoparticles and laser sintering. For a small Cu plate of 2 mm× 2 mm bonded to a larger copper substrate, a maximum shear strength of 32 MPa was achieved with a sintering pressure of 5 MPa. Although both the top surface of the substrate and the bottom surface of the chip are usually metallized with a layer of Cu, Ag or Au, the process temperatures are quite different between the pure metal plates and the metallized ceramic substrates (or the metallized semiconductor chips) due to the differences of the thermal conductivity, absorption rate and the thermal stress [29], [37], [38].

In this paper, we present the results of a laser assisted sintering method using a silver nanoparticle paste for bonding of silicon chips to DBC substrates for high temperature applications. The effects of sintering conditions on the quality of the sintered joints between the Si chips and the DBC substrates were investigated. For comparison, Si-Ag-DBC joints were also produced using a hotplate-based method. The shear strengths of the joints were measured and the cross sections and fracture surfaces were analyzed using SEM, EDS, and XRD to investigate the microstructures produced under different sintering conditions.

## II. Experiment Section

### A. Materials

In this work, the silver nanoparticle paste was Nano Tach-X material (NBE Tech LCC), which was composed of 30 nm to 50 nm range of silver nanoparticles and some micrometer-sized silver particles in organic components [37]. The dimensions of the Si chips were 4 mm× 4 mm× 0.65 mm. The dimensions of the Direct Bonded Copper (DBC) substrates were 10 mm × 10 mm × 0.65 mm. The thickness of the $Al_2O_3$ substrate was 0.625 mm and the thickness of Cu was 25 μm. The roughness of the Si surface was approximately 1 nm and the roughness of the DBC surface was 0.11 μm, which were measured using an optical surface profilometer [39].

The Si chips were metallized with a multilayer of Ti (100 nm) / Ni (100 nm) / Cu (500 nm) deposited by electron-beam evaporation. In order to remove the particles and the organic contaminations on the surfaces, the Si chips and the DBC substrates were cleaned in an ultrasonic bath using acetone, ethanol and deionized (DI) water in sequence. The Si chips and the DBC substrates were dipped in a dilute sulfuric acid solution at a volume ratio of 1:20 between $H_2SO_4$ and DI water for 30 seconds to remove the oxide on the Cu surfaces, followed by rinsing in the DI water. Subsequently, the silver nanoparticle paste layers were stencil printed onto the DBC substrates. The aperture size of the steel stencil was 4 mm× 4 mm and the thickness was 100 μm. After printing, the DBC substrates with the silver nanoparticle paste layers were preheated at 110ºC for 5 minutes to remove the organic solvents. Before sintering, the Si chips and the DBC substrates were divided into two groups. One group of samples were sintered using a hotplate-based method, while the other group were sintered using the laser assisted sintering technique.

### B. Hotplate-Based Sintering Method

In this method, the Si chip and the DBC substrate with the Ag NP layer were aligned and placed on a hotplate. Different bonding pressures of 0.3 MPa, 1.5 MPa, 3.0 MPa were applied respectively. Then, the structures were sintered at 300ºC for 30 minutes. The ramp rate of the temperature was 0.3ºC/s before reaching the sintering temperature.

### C. *Laser-Based Sintering Method*

In this method, the same Si chips and DBC substrates as for the hotplate sintering were used. However, the sintering process was carried out using a high-power diode laser system at the wavelength of 970 nm. The laser beam had a top-hat intensity distribution in a square profile of 6 mm× 6 mm. The beam delivery module consisted of collimation optics, followed by a focusing lens with a focal length of 20 cm [37], [40]-[42]. A custom designed beam forming element was placed immediately after the focusing lens to generate the top-hat beam profile. After preheating, the Si chip and the DBC substrate with the Ag NP layer were aligned and placed on the X-Y stage of the laser sintering system. Different bonding pressures of 0.3 MPa, 1.5 MPa, 3.0 MPa were applied respectively. Fig. 1 depicts the schematic of the laser-based sintering system. As shown in Fig. 1b, a thin ceramic plate was used as a thermal barrier between the DBC substrate and the steel stage in order to reduce the thermal loss. A quartz glass plate was placed on the Si chip to hold cylindrical copper blocks to apply a pressure to the bonding assembly and at the same time allowing the laser beam to reach the Si chip. The absorbed laser beam by the Si chip produced localized heating effect to increase the temperature of the nano silver layer for sintering and hence bonding the Si chip to the DBC substrate. Based on the results of our previous work in laser bonding Si substrates [37], laser powers of 60 W and 70 W were used in the laser sintering experiments respectively. Sintering times of 5 minutes, 1 minute or 30 seconds were used.

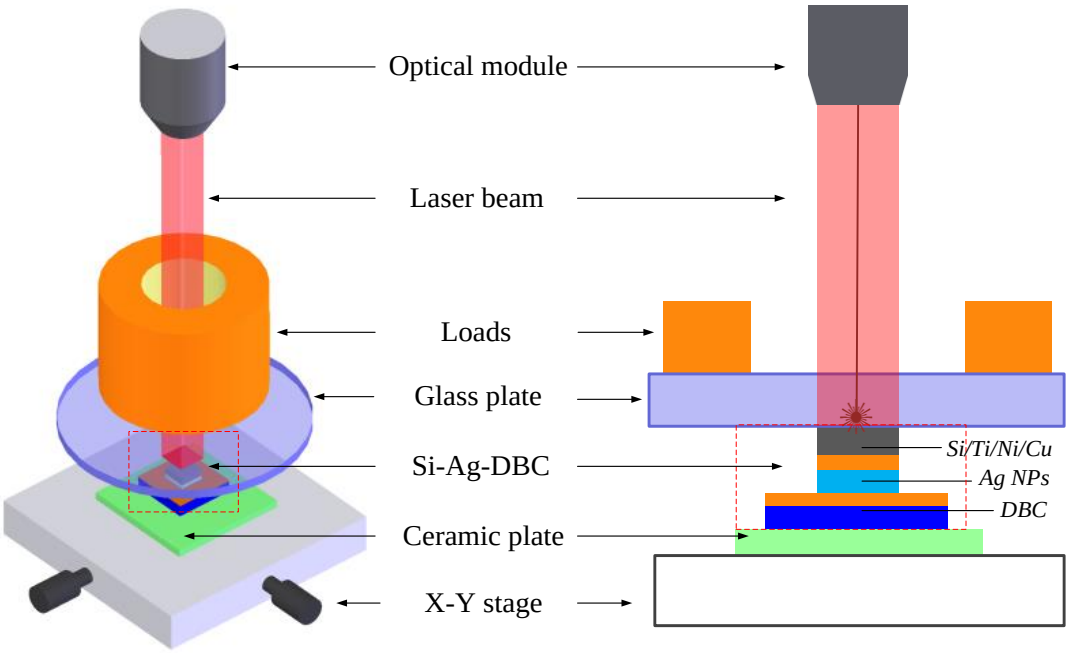


(*a*) 3D view (*b*) Cross section view

Fig. 1. Schematic of the laser-based sintering setup. (a) 3D view and (b) Cross-sectional view.

## III. Result and Discussion

### A. *Shear test*

The shear strength of the Si-Ag-DBC joints were tested using a tensile test machine (INSTRON 3367) at a rate of 5 mm/min. A purpose designed sample holder was used to mount the Si-DBC assembly in vertical configuration so shear test could be carried out on the machine. The measurement results of the shear strength tests are shown in Fig. 2.

As shown in Fig. 2a, for the hotplate-based sintering method, as the bonding pressure was increased from 0.3 MPa to 3.0 MPa, the average shear strength of three samples increased from 7.4 MPa to 12.6 MPa when the Si-Ag-DBC joints were sintered at 300ºC for 30 min. In the comparison group of laser sintered Si-Ag-DBC joints, as the bonding pressure was increased from 0.3 MPa to 3.0 MPa, the average shear strength increased from 13.7 MPa to 20.1 MPa when the samples were sintered at the laser power of 70 W for 5 min.

On one hand, these results indicate that the shear strength increases with the increasing sintering pressure. On the other hand, under the same sintering pressure, compared with the hotplate-based sintering method, higher shear strength can be obtained using the laser-based sintering method. Furthermore, the comparison of the shear strength under different laser powers and irradiation times is shown in Fig. 2b. It can be seen that the shear strength of the joints can be improved by using a higher laser power and a longer irradiation time.

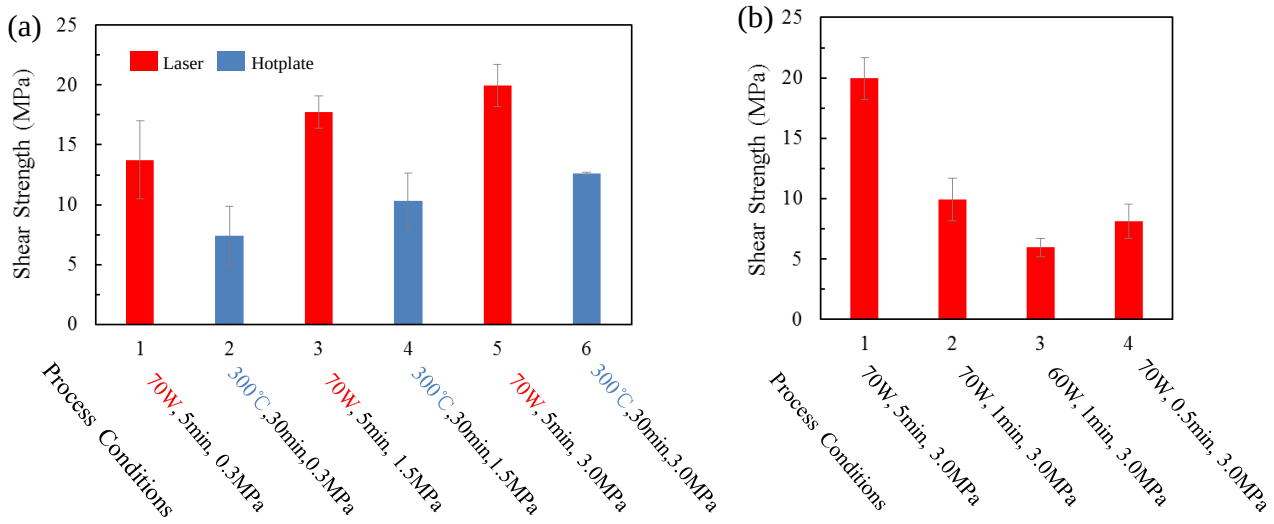


Fig. 2. Measurement results of the shear strength. (a) Comparison of shear strength of different sintering methods and pressures. Process conditions: 1. 70 W, 5 min, 0.3 MPa; 2. 300ºC, 30 min, 0.3 MPa; 3. 70 W, 5 min, 1.5 MPa; 4. 300ºC, 30 min, 1.5 MPa; 5. 70 W, 5 min, 3.0 MPa; 6. 300ºC, 30 min, 3.0 MPa. (b) Comparison of shear strength of different laser powers and times. Process conditions: 1. 70 W, 5 min, 3.0 MPa; 2. 70 W, 1 min, 3.0 MPa; 3. 60 W, 1 min, 3.0 MPa; 4. 70 W, 0.5 min, 3.0 MPa.

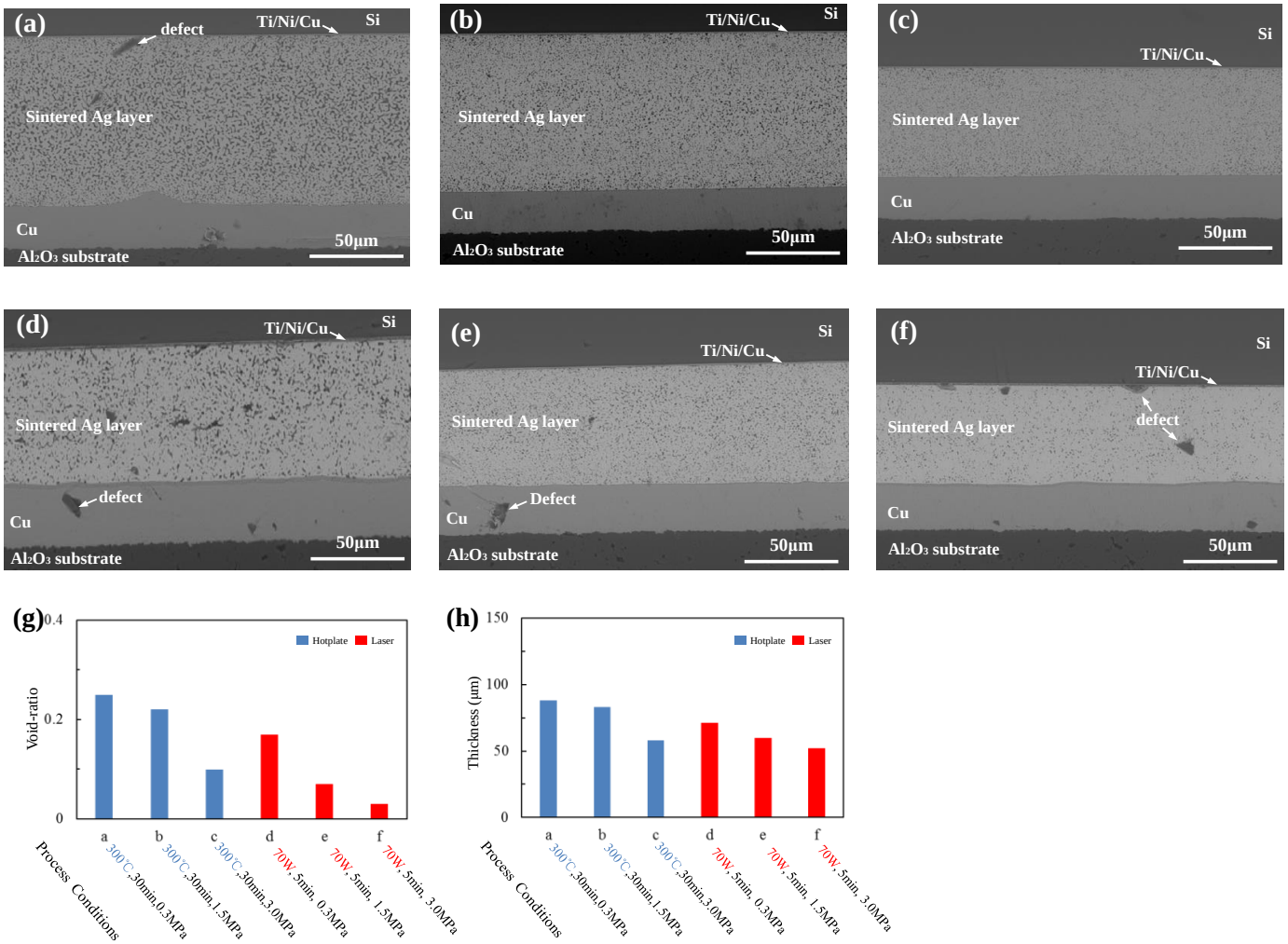


Fig. 3. SEM images of cross-sections of the Si-Ag-DBC joints. (a) Hotplate-based method, 300ºC, 30 min, 0.3 MPa; (b)

Hotplate-based method, 300ºC, 30 min, 1.5 MPa; (c) Hotplate-based method, 300ºC, 30 min, 3.0 MPa; (d) Laser-based method, 70 W, 5 min, 0.3 MPa; (e) Laser-based method, 70 W, 5 min, 1.5 MPa; (f) Laser-based method, 70 W, 5 min, 3.0 MPa; (g) The void-ratios under different process conditions; (h) The thicknesses of the sintered Ag layers under different process conditions.

### *B. Cross-sectional analysis*

In order to verify the relationship between the bonding pressure and the quality of the Si-Ag-DBC joints, the porosity of the sintered Ag layer was studied. Fig. 3 (a)-(c) show the SEM images of the cross-sections of the Ag joints sintered under different bonding pressures at 300ºC for 30 min. Fig. 3 (d)-(f) show the SEM images of the cross-sections of the joints sintered under different bonding pressures at the laser power of 70 W for 5 min. It can be seen that with the increasing sintering pressure, the sintered silver layer became denser and the large voids can be eliminated. In order to estimate the void-ratio, the gray-scale SEM images were converted to binary images and MATLAB was utilized to calculate the ratio of black areas to represent the compactness of the silver-sintered layer [43]. The defects were not taken into account. Fig. 3(g) shows the void-ratios under different process conditions. For the hotplate-based method, the void-ratio was reduced from approximately 25% for the sintering pressure of 0.3 MPa to approximately 10% for the sintering pressure of 3.0 MPa, which indicates a denser silver layer and more sintering necks [29], [37], [44]. For the laser-based method, the void-ratio was reduced from approximately 17% for the sintering pressure of 0.3 MPa to approximately 3% for the sintering pressure of 3.0 MPa. Moreover, as shown in the Fig. 3(h), the densification can also be illustrated by the reduction of the thicknesses of the sintered Ag layers, which indicates the positive effects of reducing the void-ratio by increasing the bonding pressure or using the laser-based method. Thus, the bond quality of the Si-Ag-DBC joint can be enhanced by increasing the sintering pressure.

### *C. Fracture surface analysis*

Most of the fracture surfaces were found at the interface between the sintered silver layer and the Si chip. Fig. 4a and Fig. 4b show the SEM images of the fracture surfaces of the Si-Ag-DBC joints sintered at 300ºC for 30 min at the sintering pressures of 0.3 MPa and 3.0 MPa, respectively. Fig. 4c and Fig. 4d show the SEM images of the fracture surfaces of the joints sintered at the laser power of 70 W for 5 min at the sintering pressures of 0.3 MPa and 3.0 MPa, respectively. Compared with the fracture surface in Fig. 4a for the sintering pressure of 0.3 MPa), more sintering necks were formed between the Ag NPs and a less porous sintered silver layer was obtained at a higher sintering pressure of 3.0 MPa as shown in Fig. 4b. There is a similar phenomenon in the laser sintered samples shown in Fig. 4c and Fig. 4d. Moreover, for the same sintering pressure, more sintering necks were found on the fracture surfaces of the laser sintered samples than the hotplate sintered samples, which indicate that the higher shear strength of the laser sintered samples may be due to the growth of the initial sintering necks. The growth of the sintering necks was enhanced by the fast heating rate and the relatively high temperature in the laser assisted sintering process [37], [45], [46]. The laser induced temperature in the Ag NP layer was approximately 340ºC at the power of 70 W. The temperature was measured using a small thermocouple placed between the DBC substrate and the ceramic plate, which was based on the same method as in our previous work [37]. The oxidation of the Cu surfaces of the Si and DBC can also be reduced in the rapid laser sintering method, which can facilitate the bonding between the Ag NPs and the Cu layers [47].

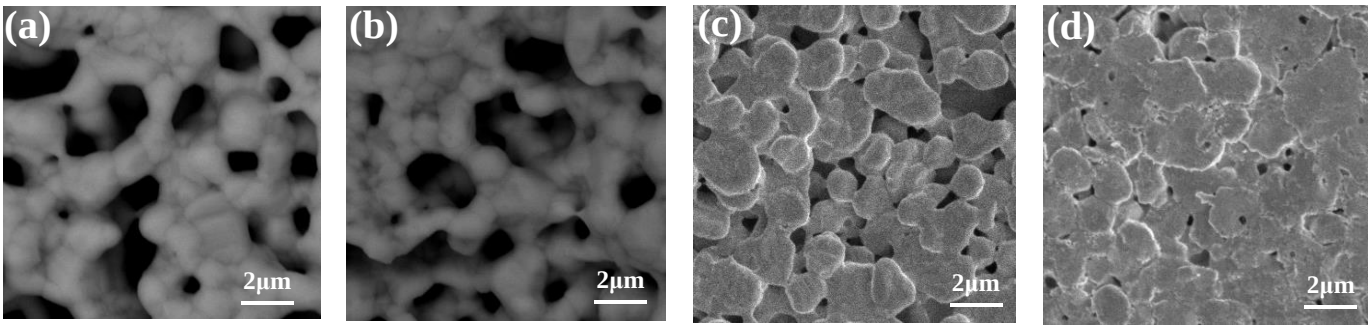


Fig. 4. SEM images of the fracture surfaces of the Si-Ag-DBC joints. (a) Hotplate-based method, 300ºC, 30 min, 0.3 MPa; (b) Hotplate-based method, 300ºC, 30 min, 3.0 MPa; (c) Laser-based method, 70 W, 5 min, 0.3 MPa; (d) Laser-based method, 70 W, 5 min, 3.0 MPa.

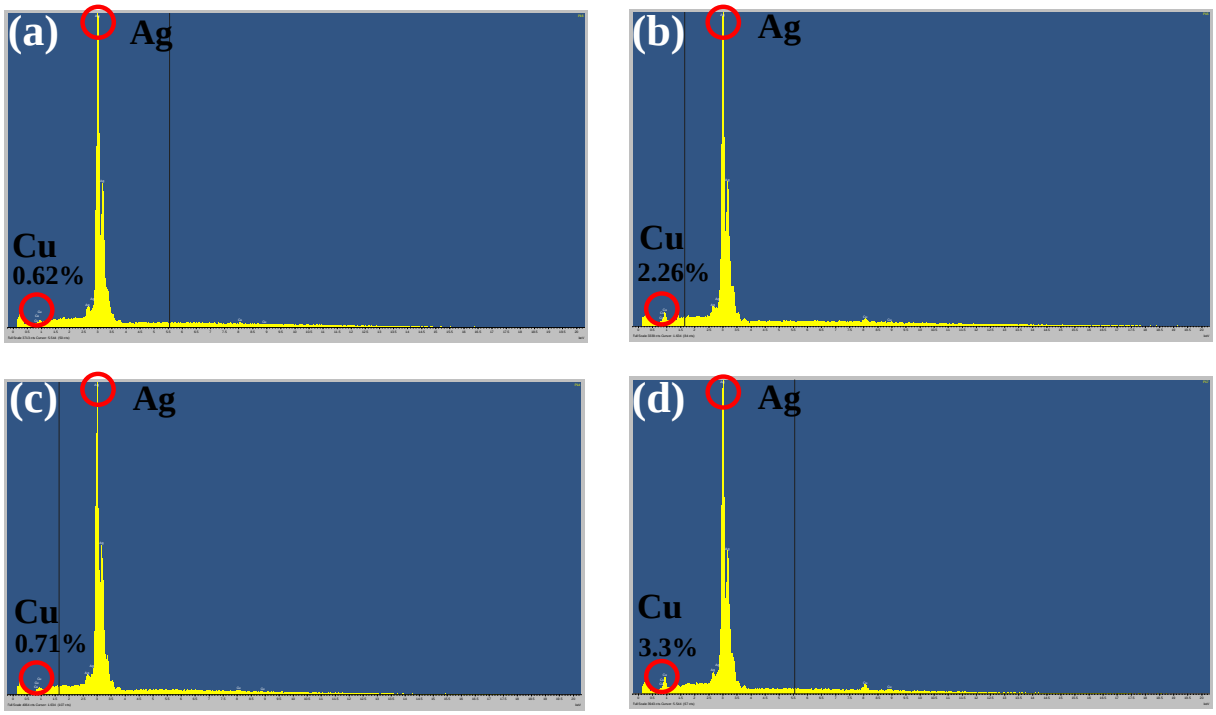


Fig. 5. EDS results of the fracture surfaces of the Si-Ag-DBC joints. (a) Hotplate-based method, 300ºC, 30 min,0.3 MPa; (b) Hotplate-based method, 300ºC, 30 min, 3.0 MPa; (c) Laser-based method, 70 W, 1 min, 3.0 MPa; (d) Laser-based method, 70 W, 5 min, 3.0 MPa.

The element composition of the fracture surfaces was analyzed using a surface energy disperse spectrometer (EDS). Fig. 5a and Fig. 5b show the EDS results of the fracture surfaces of the Si-Ag-DBC joints sintered at 300ºC for 30 min at the sintering pressures of 0.3 MPa and 3.0 MPa, respectively. Compared with the Cu content of 0.62 wt.% in Fig. 5a (sintering pressure of 0.3MPa), more Cu content of 2.26 wt.% was found for the sintering pressure of 3.0 MPa as shown in Fig. 5b. The result shows that the high sintering pressure can make the printed silver nanoparticle paste in more contact with the Cu surface of the Si chip.

The effect of the laser irradiation time on the shear strength in the results shown in Fig. 2b can be explained using the EDS results in Fig. 5c and Fig. 5d. At the same laser power of 70 W and sintering pressure of 3.0 MPa, a Cu content of 0.71 wt.% was found on the fracture surface of the sample produced with the shorter irradiation time of 1 min in Fig. 5c, while a Cu content of 3.3 wt.% could be found on the fracture surface of the sample processed with the longer irradiation time of 5 min shown in Fig. 5d. Besides, a higher Cu content was found in the laser sintered sample in Fig. 5d than the hotplate sintered sample in Fig. 5b, which indicates a better bonding quality between the Ag NPs and the Cu films using the rapid laser sintering method.

### *D. Crystal structure analysis*

Crystal structures of the Ag NPs were measured by X-ray diffraction (XRD) using Cu Kα and λ=0.15418 nm. The samples were scanned over a 2θ range of 15-85°. Samples of printed nano-Ag layers on DBC substrates were used for XRD analysis after sintering on hotplate or on the laser sintering system. The XRD patterns are shown in Fig. 6. It can be seen that the peak intensity of the Ag NPs in Fig. 6b was stronger than that in Fig. 6a. So, the Ag NPs in Fig. 6b has better crystallinity, which indicates that the laser sintering method can promote the crystallization of Ag nanoparticles. These results were consistent with the surface morphology observation in Fig. 4.

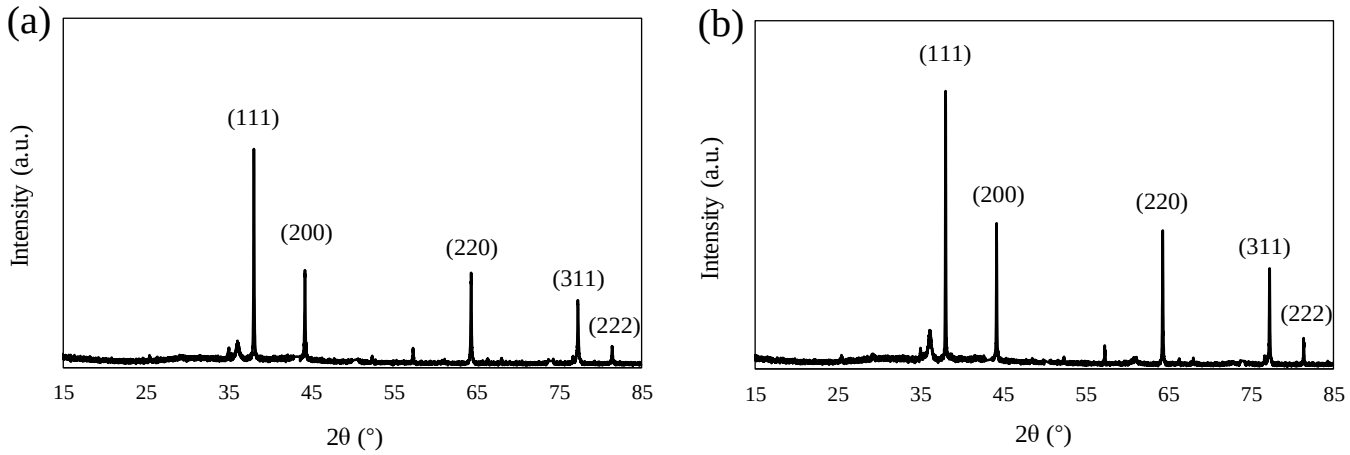


Fig. 6 XRD patterns of the Ag NPs. (a) Hotplate-based method, 300ºC, 30 min. (b) Laser-based method, 70 W, 5 min.

## IV. Conclusion

A laser assisted sintering method for a silver nanoparticle paste material for die-attach for manufacturing of high temperature electronics and sensors has been presented in this paper. The results of shear strength test show that compared with the hotplate-based sintering method, the laser assisted sintering approach can achieve better bonding quality and it is a faster technique. An average shear strength of 10 MPa can be achieved with a laser power of 70 W and an irradiation time of 1 minute. Furthermore, compared with the shear strength of approximately 5 MPa in our previous work [37] in Si-Si bonding, an average shear strength of 20.1 MPa can be obtained at a sintering/bonding pressure of 3.0 MPa, a laser power of 70W and an irradiation time of 5 minutes.

The cross sections and the fracture surfaces of the Si-Ag-DBC joints have been studies. The results of SEM and EDS analysis show that a higher sintering pressure not only makes the Ag NPs layer become denser, but also makes the printed silver nanoparticle paste in more contact with the Cu surface of the Si chip. In addition, the growth of the sintering neck size is increased with the laser power and irradiation time. Therefore, the laser assisted sintering method could meet the demands of the die-attach applications in high temperature electronics packaging.

## Acknowledgment

This work was supported by the UK Engineering and Physical Sciences Research Council (EPSRC, grant EP/R024502/1). We thank Mr. Mark Leonard for his assistance in sample preparation for cross-sectional analysis.

## References

[1] S. Guo, H. Eriksen, K. Childress, A. Fink, and M. Hoffman, "High temperature smart-cut SOI pressure sensor," *Sensors and Actuators A: Physical*, vol. 154, no. 2, pp. 255-260, 2009/09/24/ 2009.

[2] G. D. Liu *et al.*, "Silicon on insulator pressure sensor based on a thermostable electrode for high temperature applications," *Micro & Nano Letters*, vol. 10, no. 10, pp. 496-499

[3] V. M. Stuchebnikov, "SOS strain gauge sensors for force and pressure transducers," *Sensors and Actuators A: Physical*, vol. 28, no. 3, pp. 207-213, 1991/08/01/ 1991.

[4] D. J. Young, D. Jiangang, C. A. Zorman, and W. H. Ko, "High-temperature single-crystal 3C-SiC capacitive pressure sensor," *IEEE Sensors Journal*, vol. 4, no. 4, pp. 464-470, 2004.

[5] S. Arulkumaran, T. Egawa, H. Ishikawa, and T. Jimbo, "High-temperature effects of AlGaN/GaN high-electron-mobility transistors on sapphire and semi-insulating SiC substrates," *Applied Physics Letters*, vol. 80, no. 12, pp. 2186-2188, 2002.

[6] S. Yoshida and J. Suzuki, "Characterization of a GaN Bipolar Junction Transistor after Operation at 300 for over 300 h," *Japanese Journal of Applied Physics*, vol. 38, no. Part 2, No. 8A, pp. L851-L853, 1999/08/01 1999.

[7] R. S. Okojie, V. Nguyen, E. Savrun, and D. Lukco, "Improved reliability of SiC pressure sensors for long term high temperature applications," in *2011 16th International Solid-State Sensors, Actuators and Microsystems Conference*, 2011, pp. 2875-2878.

[8] V. R. Manikam and K. Y. Cheong, "Die Attach Materials for High Temperature Applications: A Review," *IEEE Transactions on Components, Packaging and Manufacturing Technology*, vol. 1, no. 4, pp. 457-478, 2011.

[9] A. Kroupa *et al.*, "Current Problems and Possible Solutions in High-Temperature Lead-Free Soldering," *Journal of Materials Engineering and Performance*, vol. 21, no. 5, pp. 629-637, 2012/05/01 2012.

[10] G. Wu, D. Xu, X. Sun, B. Xiong, and Y. Wang, "Wafer-Level Vacuum Packaging for Microsystems Using Glass Frit Bonding," *IEEE Transactions on Components, Packaging and Manufacturing Technology*, vol. 3, no. 10, pp. 1640-1646, 2013.

[11] G. Wu, D. Xu, B. Xiong, Y. Wang, Y. Wang, and Y. Ma, "Wafer-Level Vacuum Packaging for MEMS Resonators Using Glass Frit Bonding," *Journal of Microelectromechanical Systems*, vol. 21, no. 6, pp. 1484-1491, 2012.

[12] X. Chen, P. Yan, J. Tang, G. Xu, and L. Luo, "Development of wafer level glass frit bonding by using barrier trench technology and precision screen printing," *Microelectronic Engineering*, vol. 100, pp. 6-11, 2012/12/01/ 2012.

[13] A. Sharif *et al.*, "Pb-Free Glass Paste: A Metallization-Free Die-Attachment Solution for High-Temperature Application on Ceramic Substrates," *Journal of Electronic Materials*, vol. 42, no. 8, pp. 2667-2676, 2013/08/01 2013.

[14] S. W. Yoon, M. D. Glover, H. A. Mantooth, and K. Shiozaki, "Reliable and repeatable bonding technology for high temperature automotive power modules for electrified vehicles," *Journal of Micromechanics and Microengineering*, vol. 23, no. 1, p. 015017, 2012/12/13 2012.

[15] D. H. Jung, A. Sharma, M. Mayer, and J. P. Jung, "A Review on Recent Advances in Transient Liquid Phase (TLP) Bonding for Thermoelectric Power Module," in *REVIEWS ON ADVANCED MATERIALS SCIENCE* vol. 53, ed, 2018, p. 147.

[16] N. S. Bosco and F. W. Zok, "Strength of joints produced by transient liquid phase bonding in the Cu–Sn system," *Acta Materialia*, vol. 53, no. 7, pp. 2019-2027, 2005/04/01/ 2005.

[17] Y. Rong, J. Cai, S. Wang, and S. Jia, "Low temperature Cu-Sn bonding by isothermal solidification technology," in *2009 International Conference on Electronic Packaging Technology & High Density Packaging*, 2009, pp. 96-98.

[18] G. D. Liu, C. C. Gao, Y. X. Zhang, and Y. L. Hao, "High temperature pressure sensor using Cu-Sn wafer level bonding," in *2015 IEEE SENSORS*, 2015, pp. 1-4.

[19] T.-T. Luu, A. Duan, K. E. Aasmundtveit, and N. Hoivik, "Optimized Cu-Sn Wafer-Level Bonding Using Intermetallic Phase Characterization," *Journal of Electronic Materials*, vol. 42, no. 12, pp. 3582-3592, 2013/12/01 2013.

[20] R. Khazaka, L. Mendizabal, and D. Henry, "Review on Joint Shear Strength of Nano-Silver Pasteand Its Long-Term High Temperature Reliability," *Journal of Electronic Materials*, vol. 43, no. 7, pp. 2459-2466, 2014/07/01 2014.

[21] X. Li, G. Chen, L. Wang, Y.-H. Mei, X. Chen, and G.-Q. Lu, "Creep properties of low-temperature sintered nano-silver lap shear joints," *Materials Science and Engineering: A*, vol. 579, pp. 108-113, 2013/09/01/ 2013.

[22] C. Chen *et al.*, "Mechanical Deformation of Sintered Porous Ag Die Attach at High Temperature and Its Size Effect for Wide-Bandgap Power Device Design," *Journal of Electronic Materials*, vol. 46, no. 3, pp. 1576-1586, 2017/03/01 2017.

[23] Y. Tan, X. Li, and X. Chen, "Fatigue and dwell-fatigue behavior of nano-silver sintered lap-shear joint at elevated temperature," *Microelectronics Reliability*, vol. 54, no. 3, pp. 648-653, 2014/03/01/ 2014.

[24] W. Liu *et al.*, "Recent Progress in Rapid Sintering of Nanosilver for Electronics Applications," *Micromachines*, vol. 9, no. 7, p. 346, 2018.

[25] H. Zhang *et al.*, "Effects of Sintering Pressure on the Densification and Mechanical Properties of Nanosilver Double-Side Sintered Power Module," *IEEE Transactions on Components, Packaging and Manufacturing Technology*, vol. 9, no. 5, pp. 963-972, 2019.

[26] J. Yan *et al.*, "Sintering Bonding Process with Ag Nanoparticle Paste and Joint Properties in High Temperature Environment," *Journal of Nanomaterials*, vol. 2016, pp. 1-8.

[27] T. G. Lei, J. N. Calata, G. Lu, X. Chen, and S. Luo, "Low-Temperature Sintering of Nanoscale Silver Paste for Attaching Large-Area (>100mm$^2$) Chips," *IEEE Transactions on Components and Packaging Technologies*, vol. 33, no. 1, pp. 98-104, 2010.

[28] C. Buttay *et al.*, "Die Attach of Power Devices Using Silver Sintering – Bonding Process Optimisation and Characterization," *Additional Conferences (Device Packaging, HiTEC, HiTEN, & CICMT)*, vol. 2011, no. HITEN, pp. 000084-000090, 2011/01/01 2011.

[29] F. Yu, R. W. Johnson, and M. C. Hamilton, "Process Optimization of Pressure-Assisted Rapid Ag Sintering Die Attach for 300 °C Applications," *IEEE Transactions on Components, Packaging and Manufacturing Technology*, vol. 7, no. 6, pp. 855-861, 2017.

[30] K. An, S. Hong, S. Han, H. Lee, J. Yeo, and S. H. Ko, "Selective Sintering of Metal Nanoparticle Ink for Maskless Fabrication of an Electrode Micropattern Using a Spatially Modulated Laser Beam by a Digital Micromirror Device," *ACS Applied Materials & Interfaces*, vol. 6, no. 4, pp. 2786-2790, 2014/02/26 2014.

[31] N. Alayli, F. Schoenstein, A. Girard, K. L. Tan, and P. R. Dahoo, "Spark Plasma Sintering constrained process parameters of sintered silver paste for connection in power electronic modules: Microstructure, mechanical and thermal properties," *Materials Chemistry and Physics*, vol. 148, no. 1, pp. 125-133, 2014/11/14/ 2014.

[32] Z. A. Munir, D. V. Quach, and M. Ohyanagi, "Electric Current Activation of Sintering: A Review of the Pulsed Electric Current Sintering Process," *Journal of the American Ceramic Society*, vol. 94, no. 1, pp. 1-19, 2011/01/01 2011.

[33] J. Hebb *et al.*, "Laser spike annealing for nickel silicide formation," in *2011 IEEE/SEMI Advanced Semiconductor Manufacturing Conference*, 2011, pp. 1-6.

[34] Y. Wang *et al.*, "Dual beam laser spike annealing technology," in *2010 International Workshop on Junction Technology Extended Abstracts*, 2010, pp. 1-6.

[35] J. Mileham, J. Willis, D. M. Owen, S. Shetty, J. Hebb, and Y. Wang, "Impact of pattern and LSA stitching effects and processing parameters on reflectance and stress distribution for thermal annealing technologies," in *2009 17th International Conference on Advanced Thermal Processing of Semiconductors*, 2009, pp. 1-6.

[36] Y. S. Lee *et al.*, "Laser-Sintered Silver Nanoparticles as a Die Adhesive Layer for High-Power Light-Emitting Diodes," *IEEE Transactions on Components, Packaging and Manufacturing Technology*, vol. 4, no. 7, pp. 1119-1124, 2014.

[37] W. Liu, C. Wang, C. Wang, X. Jiang, and X. Huang, "Laser Sintering of Nano-Ag Particle Paste for High-Temperature Electronics Assembly," *IEEE Transactions on Components, Packaging and Manufacturing Technology*, vol. 7, no. 7, pp. 1050-1057, 2017.

[38] W. Liu *et al.*, "Laser sintering mechanism and shear performance of Cu–Ag–Cu joints with mixed bimodal size Ag nanoparticles," *Journal of Materials Science: Materials in Electronics*, vol. 30, no. 8, pp. 7787-7793, 2019/04/01 2019.

[39] M. Wang, Y. Mei, X. Li, R. Burgos, D. Boroyevich, G. Q. Lu, How to determine surface roughness of copper substrate for robust pressureless sintered silver in air, *Materials Letters*, 228 (2018) 327-330.

[40] Y. Liu, J. Zeng, and C. Wang, "Accurate Temperature Monitoring in Laser-Assisted Polymer Bonding for MEMS Packaging Using an Embedded Microsensor Array," *Journal of Microelectromechanical Systems*, vol. 19, no. 4, pp. 903-910, 2010.

[41] X. Jiang, S. Chandrasekar, and C. Wang, "A laser microwelding method for assembly of polymer based microfluidic devices," *Optics and Lasers in Engineering*, vol. 66, pp. 98-104, 2015/03/01/ 2015.

[42] J. Mileham, J. Willis, D.M. Owen, S. Shetty, J. Hebb, Y. Wang, Impact of pattern and LSA stitching effects and processing parameters on reflectance and stress distribution for thermal annealing technologies, 2009 17th International Conference on Advanced Thermal Processing of Semiconductors, 2009, pp. 1-6.

[43] M. Abbasgholipourghadim et al., “Porosity prediction of hollow fiber membrane incorporating neural network and digital image processing,” in Proc. 6th Int. Conf. Fluid Mech. Heat Mass Transfer (FLUIDSHEAT), Malaysia, Apr. 2015, pp. 113–117.

[44] F. Yu, J. Cui, Z. Zhou, K. Fang, R. W. Johnson, and M. C. Hamilton, "Reliability of Ag Sintering for Power Semiconductor Die Attach in High-Temperature Applications," *IEEE Transactions on Power Electronics*, vol. 32, no. 9, pp. 7083-7095, 2017.

[45] P. Peng, A. Hu, and Y. Zhou, "Laser sintering of silver nanoparticle thin films: microstructure and optical properties," *Applied Physics A*, vol. 108, no. 3, pp. 685-691, 2012/09/01 2012.

[46] S. Jiang, Y. Zhang, Y. Gan, Z. Chen, and H. Peng, "Molecular dynamics study of neck growth in laser sintering of hollow silver nanoparticles with different heating rates," *Journal of Physics D: Applied Physics*, vol. 46, no. 33, p. 335302, 2013/07/29 2013.

[47] S. T. Chua and K. S. Siow, "Microstructural studies and bonding strength of pressureless sintered nano-silver joints on silver, direct bond copper (DBC) and copper substrates aged at 300 °C," *Journal of Alloys and Compounds*, vol. 687, pp. 486-498, 2016/12/05/ 2016.